Electronic Supplementary Material (ESI) for EES Catalysis.

Supporting Information

Two-step Tandem Electrochemical Conversion of Oxalic Acid and Nitrate to Glycine

Yuan-Zi Xu, Daniel F. Abbott, Lok Nga Poon, Victor Mougel[*]

Department of Chemistry and Applied Biosciences, ETH Zürich, 8093 Zürich (Switzerland).

E-mail: mougel@inorg.chem.ethz.ch

Table of Contents

Experimental Details

Materials

Glycine (≥98%), sulfuric acid (≥98%), sodium nitrate (>99.0%), nitric acid (>65%), and dimethylsulfoxide-d^6 (99.8 at.% D) were purchased from Sigma Aldrich. Lead foil (99.9995%, 1 mm thick) and NH_4Cl (99.999%) were purchased from Alfa Aesar. Oxalic acid dihydrate (≥99%), maleic acid (>99.0%) and glycolic acid (99%) were purchased from Acros. Glyoxylic acid (≥95%) was purchased from Fluorochem; Hydroxylamine (50% aqueous solution) was purchased from ABCR. All chemicals were used without further purification. Electrolyte solutions were prepared with ultrapure water (Barnstead™ GenPure™ xCAD Plus Ultrapure Water Purification System, Thermo Scientific).

Electrode preparation and characterization

A fresh piece of Pb foil (1×1 cm^2) was immersed in 20% (v/v) nitric acid solution for 1 min, rinsed with Milli-Q water, and then dried under Ar. The morphology and surface composition of the treated Pb foil were characterized (Figure S2) by scanning electron microscopy (SEM) and energy-dispersive X-ray spectroscopy (EDX) using a thermal field-emission scanning electron microscope (JEOL JSM7100F).

Electrochemical measurements

All electrochemical measurements were conducted using a VSP-300 (Bio-Logic Science Instruments) potentiostat. A piece of pre-treated lead foil (1×1 cm^2; see above for preparation) was used as the working electrode, a platinum wire served as the counter electrode, and an Ag/AgCl (3M NaCl) was used as the reference electrode. All measured potentials were converted to the reversible hydrogen electrode (RHE) scale using the formula below:

$$E(\text{V vs. RHE}) = E(\text{V vs. Ag/AgCl}) + 0.059 \times \text{pH} + 0.209$$

Electrolysis experiments were carried out in a glass, 2-compartment H-type cell. The anode and cathode chambers were separated by a piece of Nafion 211 membrane and the cell inlets/outlets were sealed with gas-tight Teflon caps. The cell was connected to a gas chromatograph (SRI Instruments 8610C) for on-line detection of gaseous products in the headspace. The catholyte and anolyte volume were always kept at 10 and 12 mL, respectively. Unless otherwise mentioned, the anolyte in all experiments was 0.5 M H_2SO_4.

Detailed procedures of the different tandem strategies investigated in the present work are given below, and optimized conditions are schematically illustrated in Scheme S1:

One-step tandem electrolysis experiments: a catholyte solution containing 0.5 M oxalic acid and 0.5 M $NaNO_3$ was used. Prior to electrolysis this catholyte solution was degassed with argon for 30 minutes to remove dissolved oxygen. Chronopotentiometry (i.e. constant current electrolysis) was performed over a range of -50 to -600 mA cm^{-2} for 30 minutes each at each current density.

Using that setup, the influence of the presence of sulfuric acid in the catholyte was investigated via recording linear sweep voltammograms (LSVs) of the Pb foil at 10 mV s^{-1} in a 0.5 M oxalic acid and 0.5 M $NaNO_3$ catholyte solution with and without 0.5 M H_2SO_4, prior to carrying out chronopotentiometry under the same conditions at a constant current density of -200 mA cm^{-2}.

Two-step tandem electrolysis (same *j*) experiments: a catholyte solution containing 0.5 M oxalic acid was used for the first step (i.e. oxalic acid to glycolic acid step). Prior to electrolysis this catholyte solution was degassed with argon for 30 minutes to remove dissolved oxygen. Chronopotentiometry was then conducted for 30 minutes at a given current density, ranging between -50 and -600 mA cm^{-2}.

Afterwards, solid $NaNO_3$ was added directly to the catholyte under positive argon flow to bring the NO_3^- concentration to 0.5 M. Chronopotentiometry was then pursued at the same current density for an additional 30 minutes.

Two-step tandem electrolysis (optimized *j*) experiments: a catholyte solution containing 0.5 M oxalic acid was used for the first step (i.e. oxalic acid to glycolic acid step). Prior to electrolysis this catholyte solution was degassed with argon for 30 minutes to remove dissolved oxygen. Chronopotentiometry was then conducted for 30 minutes at -500 mA cm^{-2}.

Afterwards, solid $NaNO_3$ was added directly to the catholyte under positive argon flow to bring the NO_3^- concentration to 0.5 M. Chronopotentiometry was then pursued for 30 minutes at a constant current density ranging from -50 to -400 mA cm^{-2}.

Quantification of liquid products

The liquid products and intermediates were analysed using ^1H nuclear magnetic resonance (^1H NMR) spectroscopy on a Bruker Avance Spectrometer, operating at a proton frequency of 500.06 MHz (AVIII-500, Burlingame, CA, USA). Water suppression was achieved using excitation sculpting (WATERGATE) with a perfect-echo pulse sequence. The 1H NMR experiments were conducted with the following optimized parameters: pulse width of 2.4 µs; 64 K data points; 128 scans; acquisition time of 7.27 s; and spectral width of 0.230 Hz. Key products and intermediates, including glycine, NH_3, glycolic acid, and glyoxylic acid, were directly analysed using ^1H NMR. Additionally, glyoxylic oxime, synthesized by reacting glycolic acid with hydroxylamine, was quantified. Hydroxylamine was detected indirectly through its condensation with excess formaldehyde to form formaldoxime.[1, 2] For calibration, standard solutions of each compound were prepared at concentrations of 1, 5, 10, 25, and 50 mM in deionized water, with the pH adjusted to approximately 2 using dilute H_2SO_4. An internal standard was prepared by dissolving 0.29 g of maleic acid in 10 mL of DMSO-d_6. Then, 0.45 mL of the sample was mixed with 50 µL of the DMSO-d_6/maleic acid solution in an NMR tube for NMR analysis. Calibration curves were constructed by plotting the peak area ratio of analyte signals to the maleic acid vinylic singlet (6.27 ppm, 2H) against concentration. For hydroxylamine, its concentration was determined indirectly by measuring the ^1H NMR signal of the trans-H peak of formaldoxime, which appears at approximately 7.00 ppm. In the concentration range of 1–50 mM, the integrated areas of all fitted curves of standard solutions of the products showed a strong linear relationship with the concentrations. Linear fits of these calibration curves (**Figures S3-8**) were used for concentration determination.

For electrolyte analysis, post-reaction samples were diluted 9-fold with deionized water, and the pH was adjusted to approximately 2. A 0.45 mL aliquot of the diluted electrolyte was mixed with 50 µL of the DMSO-d_6/maleic acid internal standard in an NMR tube for NMR measurement. Quantification of the reaction products was performed by comparing the integral area of their characteristic NMR peaks to the vinylic singlet of maleic acid, using the pre-established calibration curves.

The faradaic efficiency (FE) towards the potential products can then be calculated as:

$$\mathrm{FE} = \frac{\mathrm{n \cdot F \cdot c \cdot V}}{\mathrm{Q}} \times 100\%$$

where n represents the number of electrons required for the formation of products in oxalic acids reduction (n=2 for formation of glyoxylic acid, n=4 for formation of glycolic acid in one-step electrolysis, n=2 for formation of glycolic acid in two-step tandem electrolysis, n=6 for formation of glyoxylic acid oxime, n=6 for formation of hydroxylamine, n=10 for formation of glycine in two-step tandem electrolysis, n=12 for formation of glycine in one-step electrolysis), F = 96485 C $\mathrm{mol^{-1}}$, c is the concentration for products in mol $\mathrm{L^{-1}}$, V is the volume of the electrolyte in liters, and Q is the total charge transferred through the working electrode in coulombs.

Yield rate of glycine were determined according to the formula below:

$$\mathrm{R} = \frac{\mathrm{c \cdot V}}{\mathrm{t \cdot A}}$$

Where A correspond to the electrode geometric area (here 1 $\mathrm{cm^2}$).

Partial current density of j_{glycine} is calculated by multiplying the total current j_{total} with the faradaic efficiency $\mathrm{FE_{glycine}}$ as shown in equation below.

$$j_{\mathrm{glycine}} = j_{\mathrm{total}} \cdot \mathrm{FE_{glycine}}$$

The conversion of oxalic acid to glyoxylic acid or glyoxylic acid to glycine was calculated using the equation below:

$$\mathrm{R} = \frac{C_1}{C_0}$$

where the C_1 represents the concentration of glyoxylic acid in the oxalic acid to glyoxylic acid step (step 1) or glycine in the glyoxylic acid to glycine step (step 2) after electrolysis, C_0 is the initial concentration of oxalic acid in the oxalic acid to glyoxylic acid step (step 1) or glyoxylic acid in the glyoxylic acid to glycine step (step 2). The overall conversion of oxalic acid to glycine was calculated by multiplying the conversion of oxalic acid to glyoxylic acid by the conversion of glyoxylic acid to glycine in the two-step tandem electrolysis.

Note: It is worth noting that at current densities exceeding -300 mA $\mathrm{cm^{-2}}$, a minor quantity of formic acid is produced. Nevertheless, the faradaic efficiency of formic acid is less than 1%. Therefore, this product is not discussed in the main text.

Quantification of gaseous products

Hydrogen gas was quantified using a gas chromatograph (GC) (SRI, 8610C) equipped with a 9' 5 Å molecular sieves column, a helium ion detector (HID) and a thermal conductivity detector (TCD) and He carrier gas with 10 mL min^{-1}. For each 30-minute electrolysis, 3 separate injections of 1 mL of the headspace gas were injected over 12 s, with a 1-minute break between the end of each GC measurement and the next injection. Consequently, an averaged value for each CA measurement was obtained. The FE was calculated using the following equation.

$$\mathrm{FE(H_2)}=\frac{F\cdot N\cdot n}{Q}$$

Where F is again the Faraday's constant (96485 C mol^{-1}), N is the number of moles of product measured, n is number of electrons transferred (n = 2 for H_2), and Q is the amount of charge transferred during the time of the gas injection (12 s).

Supporting Tables

Table S1. Standard Gibbs free energy of formation ($\Delta_f G°$) values used for the calculation of the standard reduction potentials (E°) shown in Table S2 and Scheme 1b. Thermodynamics data was obtained from www.chemeo.com.

	$\Delta_f G°$ (kJ/mol)
$\Delta_f G°_{\text{oxalic acid}}$	-565.52
$\Delta_f G°_{\text{glyoxylic acid}}$	-399.30
$\Delta_f G°_{\text{glycolic acid}}$	-436.60
$\Delta_f G°_{H2O}$	-228.80

Table S2. Standard Gibbs free energy change (ΔG°) and the standard reduction potentials (E°) of species involved in the tandem glycine electrosynthesis (using the thermodynamic cycles in **Figure S1**, we can calculate the ΔG° and E° for individual reactions).

	ΔG° (kJ/mol)		E° (V vs. SHE)
$\Delta G°_1$ [(a)]	70	$E°_1$ [(a)]	-0.363
$\Delta G°_2$ [(a)]	-43.6	$E°_2$ [(a)]	0.226
$\Delta G°_3$ [(a)]	26.4	$E°_3$ [(a)]	-0.068
$\Delta G°_4(HNO_3/N_2)$ [(b)]	-601.102	$E°_4(HNO_3/N_2)$ [(b)]	1.246
$\Delta G°_5(HNO_3/NH_3OH^+)$ [(b)]	-420.867	$E°_5(HNO_3/NH_3OH^+)$ [(b)]	0.727
$\Delta G°_6(HNO_3/NH_4^+)$ [(b)]	-680.026	$E°_6(HNO_3/NH_4^+)$ [(b)]	0.881
$\Delta G°_6(NH_3OH^+/NH_4^+)$ [(b)]	-259.185	$E°_6(NH_3OH^+/NH_4^+)$ [(b)]	1.343

[(a)] The data compiled in this work utilize the values from **Table S1**, with calculations obtained from www.chemeo.com.

[(b)] The data were sourced and calculated from the referenced papers.[3, 4]

Table S3. Cell resistance values at different H_2SO_4 concentrations of anolyte in the oxalic acid to glyoxylic acid step and in the glyoxylic acid oxime to glycine step.

anolyte	1M H_2SO_4	0.5M H_2SO_4	0.1M H_2SO_4
oxalic acid to glyoxylic acid	0.515 Ω	1.441 Ω	2.942 Ω
glyoxylic acid oxime to glycine	0.467 Ω	1.252 Ω	2.231 Ω

Table S4. Comparison of glycine faradaic efficiency, current density, and yield rate for selected glycine electrosynthesis processes.

Catalysts	**Catholyte**	**Anolyte**	**FE (%)**	**$j_{glycine}$ (mA·cm^{-2})**	**Yield rate (mmol h^{-1} cm^{-2})**	**Ref.**
Pb foil	*0.5 M oxalic acid in 1st step (-500 mA cm^{-2}); 0.5 M $NaNO_3$ added for 2nd step (-400 mA cm^{-2}) - Two-step tandem electrolysis (optimized j)*	*0.5M H_2SO_4*	*59.5 ± 6.4*	*-226 ± 25.5*	*0.82 ± 0.1*	*This work*
Pb foil	*0.5 M oxalic acid in 1st step (-500 mA cm^{-2}); 0.5 M $NaNO_3$ added for 2nd step (-400 mA cm^{-2}) - Two-step tandem electrolysis (optimized j)*	*0.5M H_2SO_4*	*61.5 ± 5.7*	*-166.5 ± 19.1*	*0.6 ± 0.05*	*This work*
Cu-Hg	15 wt % H_2SO_4 solution containing 0.25 M oxalic acid and 0.25 M $NaNO_3$	-	43.1	-90	-	[5]
Pb foil	15 wt % H_2SO_4 solution containing 0.25 M oxalic acid and 0.25 M $NaNO_3$	-	10	-	-	[5]
$Pb_1Bi_{0.1}$	1.5 M H_2SO_4 solution containing 0.25 M oxalic acid and 0.25 M $NaNO_3$	*1.5M H_2SO_4*	46.1	-635.5	1.25	[6]
PbSnBi	1.5 M H_2SO_4 solution containing 0.25 M oxalic acid and 0.25 M $NaNO_3$	*1.5M H_2SO_4*	57.2	-572	1.125	[7]
PbCu	0.1 M K_2SO_4 solution containing 0.2 M H_2SO_4, 0.25 M oxalic acid, and 0.25 M NH_2OH	-	78	-156	-	[8]
Fe–N–C-700	0.5 M oxalic acid and 0.5 M $NaNO_3$		64.2	-106		[9]
$CuPb_{1ML}$	0.5M oxalic acid and 0.5 M $NaNO_3$	-	57	-144	-	[10]
TiO_2/Ti mesh	0.1 M H_2SO_4 solution containing 0.25 M oxalic acid and 0.25 M NH_2OH	-	96	-	-	[11]
CNTs	0.2 M H_2SO_4 solution containing 160 mM glyoxylic acid and 80 mM $(NH_2OH)_2 \cdot H_2SO_4$	-	87.4	-94.965	-0.34 *	[12]
CoFe-SSM	60 mM glyoxylic acid, 6 M ammonia	-	41.2	-30.86	-	[13]
Ti foil	0.1 M HCl solution containing 40 mM glyoxylic acid, 15 mL min^{-1} NO	-	28	-1.33	-	[14]
OD-Ag	0.5 M H_2SO_4 solution containing 160 mM oxalic acid and 96 mM $(NH_2OH)_2 \cdot H_2SO_4$	-	21	-	-	[15]
AD-Fe/NC	0.5 M PBS containing glyoxylic acid and NO	-	12.6	-	0.00447	[16]
Ti felt	0.1 M HCl solution containing 20 mM glyoxylic acid, 20 mL min^{-1} NO gas	-	-	-	0.28	[17]

* estimated according to the provided $j_{glycine}$, as the yield rate was only provided in mmol h^{-1} mg^{-1} in the original study.

Table S5. Composition of cathode electrolyte after long-term electrolysis.

Glycine[a]	NH_3[a]	Glyoxylic acid[a]	Oxalic acid[b]	Glycolic acid[a]	Glyoxylic oxime[a]	NH_2OH[a]	Nitrate[c]
175mM	153mM	103mM	79mM	13.3mM	10mM	5mM	79mM

[a] determined by ^{1}H NMR; [b] determined by UV-Vis titration; [c] determined by ionic chromatography.

Supporting Figures

Scheme S1. Schematic illustration of the two-step tandem electrochemical conversion of oxalic acid and nitrate to glycine, depicting the experimental conditions and setup and the sequential electrochemical transformations.

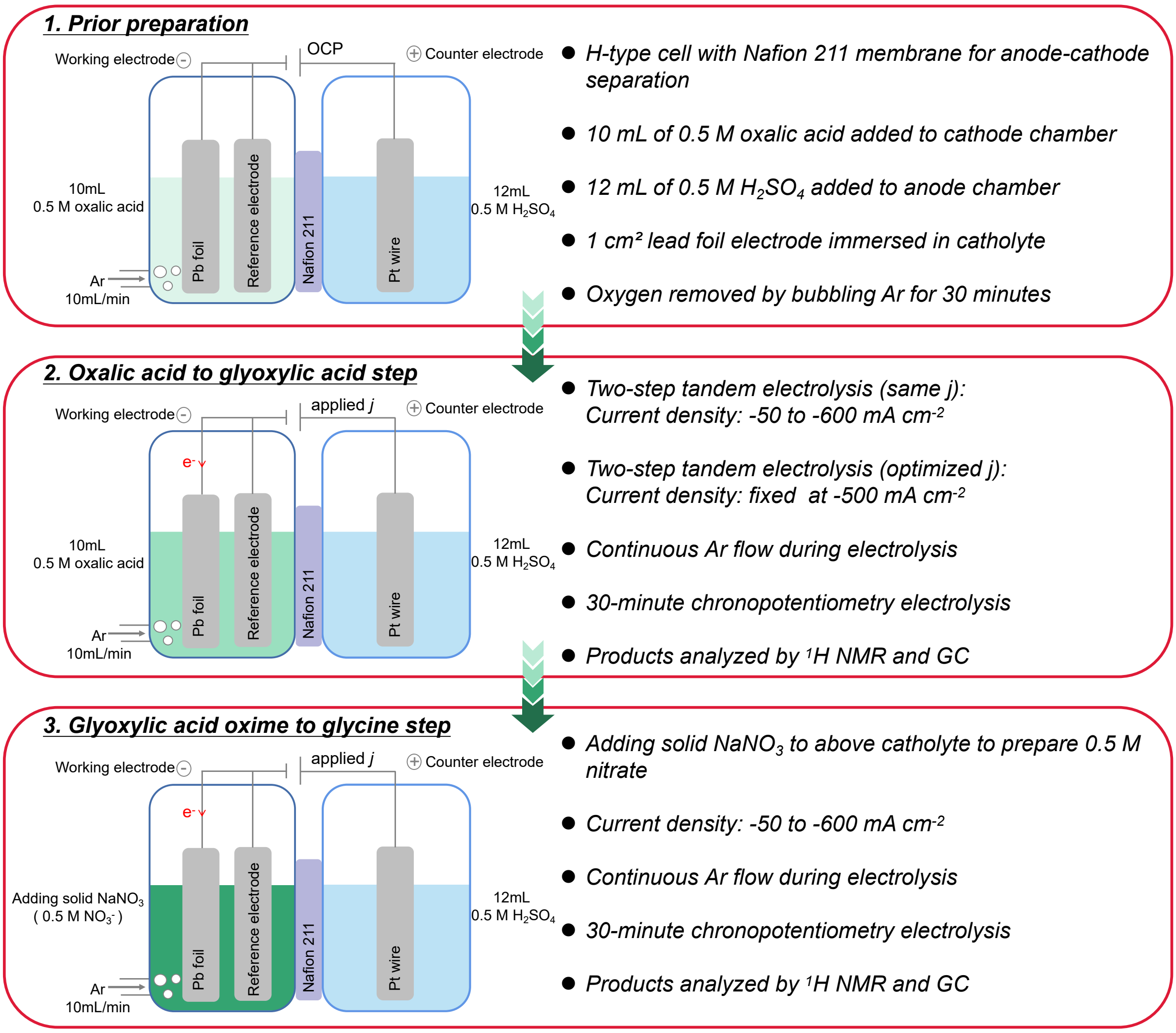

1. Prior preparation

- *H-type cell with Nafion 211 membrane for anode-cathode separation*
- *10 mL of 0.5 M oxalic acid added to cathode chamber*
- *12 mL of 0.5 M H_2SO_4 added to anode chamber*
- *1 cm² lead foil electrode immersed in catholyte*
- *Oxygen removed by bubbling Ar for 30 minutes*

2. Oxalic acid to glyoxylic acid step

- *Two-step tandem electrolysis (same j): Current density: -50 to -600 mA cm^{-2}*
- *Two-step tandem electrolysis (optimized j): Current density: fixed at -500 mA cm^{-2}*
- *Continuous Ar flow during electrolysis*
- *30-minute chronopotentiometry electrolysis*
- *Products analyzed by ^{1}H NMR and GC*

3. Glyoxylic acid oxime to glycine step

- *Adding solid $NaNO_3$ to above catholyte to prepare 0.5 M nitrate*
- *Current density: -50 to -600 mA cm^{-2}*
- *Continuous Ar flow during electrolysis*
- *30-minute chronopotentiometry electrolysis*
- *Products analyzed by ^{1}H NMR and GC*

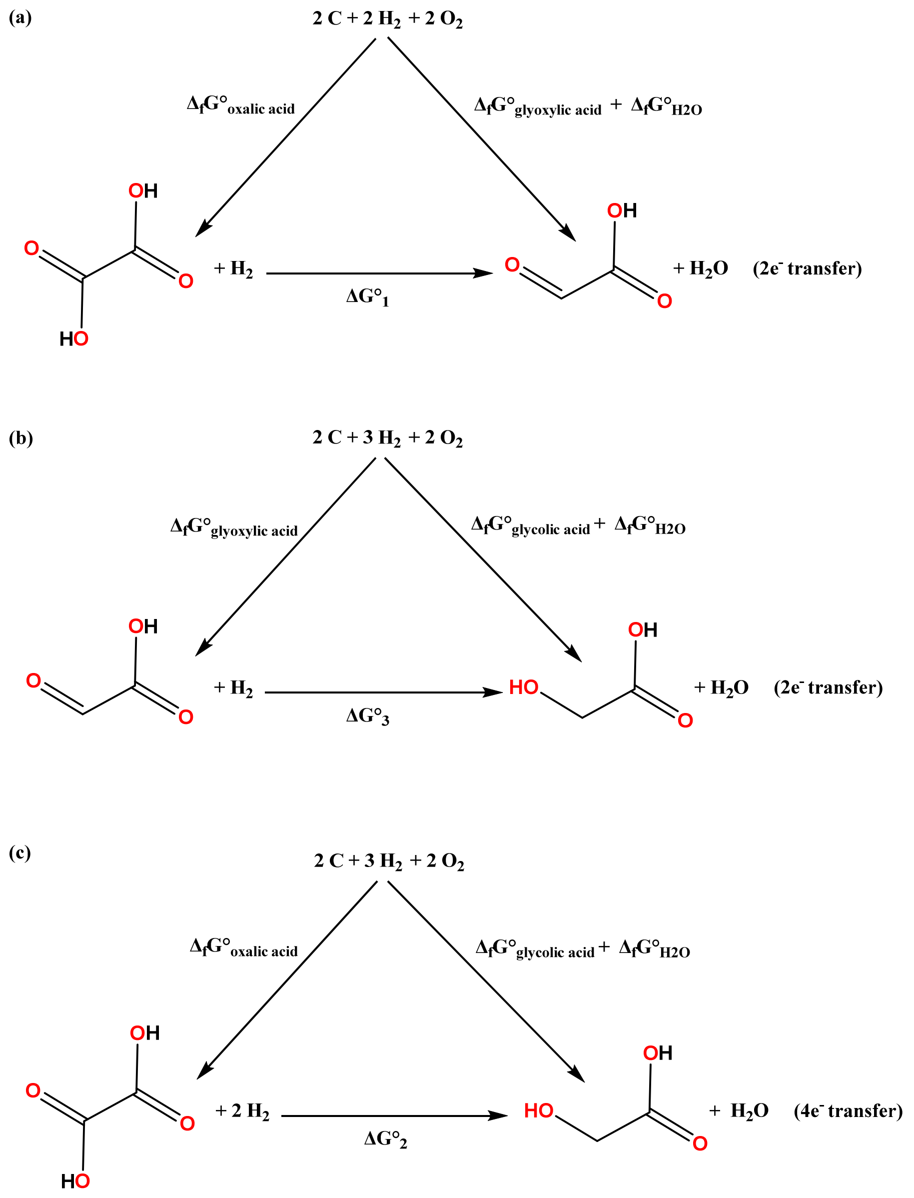

Figure S1. Hess cycles used for calculating the standard Gibbs free energy changes associated with the formation of compounds (*cf.* Table S2).

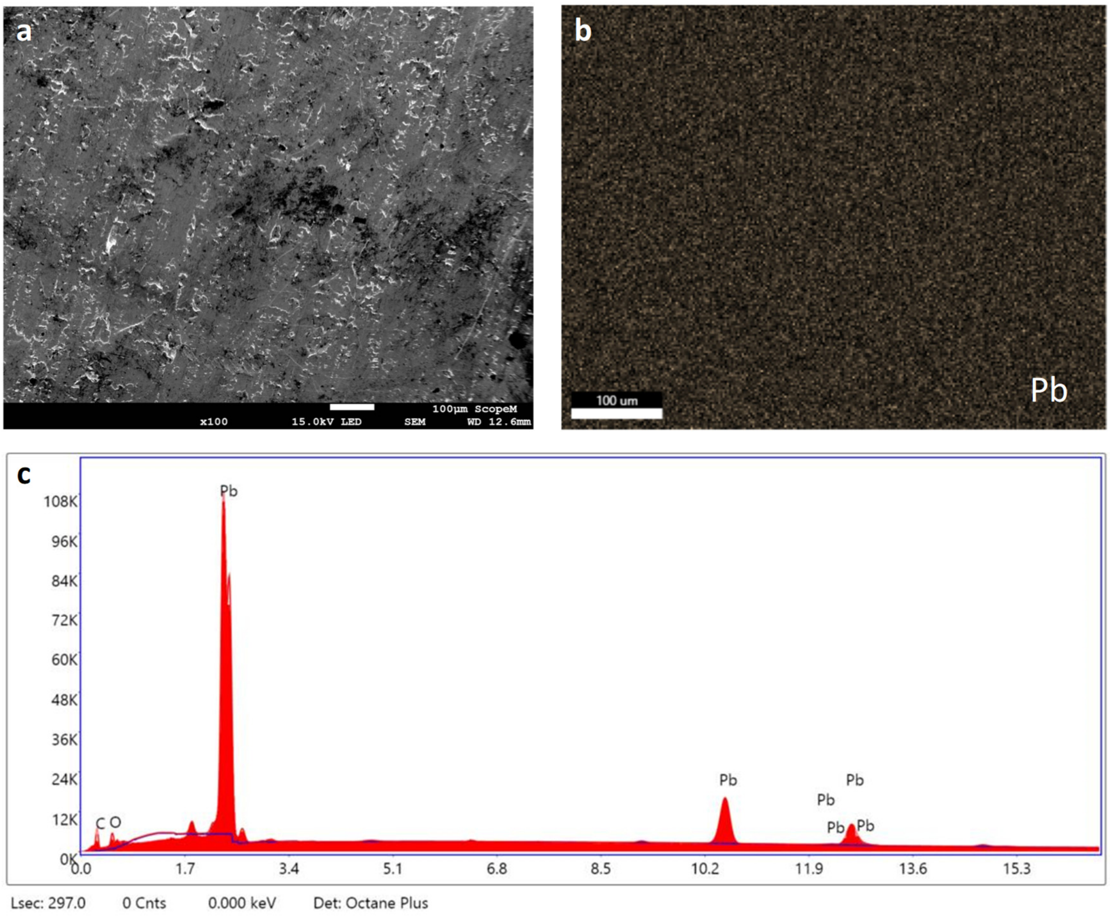

Figure S2. (a) SEM micrograph and the corresponding (b) EDX map and (c) EDX spectrum of the Pb foil electrode after the cleaning treatment in nitric acid.

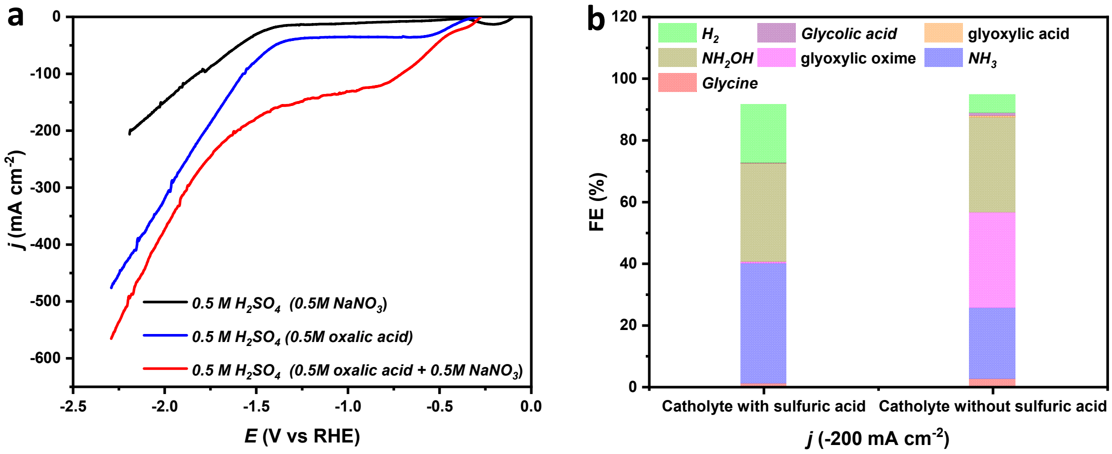

Figure S3. (a) Linear sweep voltammograms collected at 10 mV s^{-1} of Pb foil in 0.5 M H_2SO_4 containing 0.5 M oxalic acid, 0.5 M $NaNO_3$, or 0.5 M oxalic acid and 0.5 M $NaNO_3$. (b) Influence of the presence of 0.5 M H_2SO_4 in the catholyte solution on the product distribution during the one-pot, one-step electrolysis at -200 mA cm^{-2} for 30 minutes.

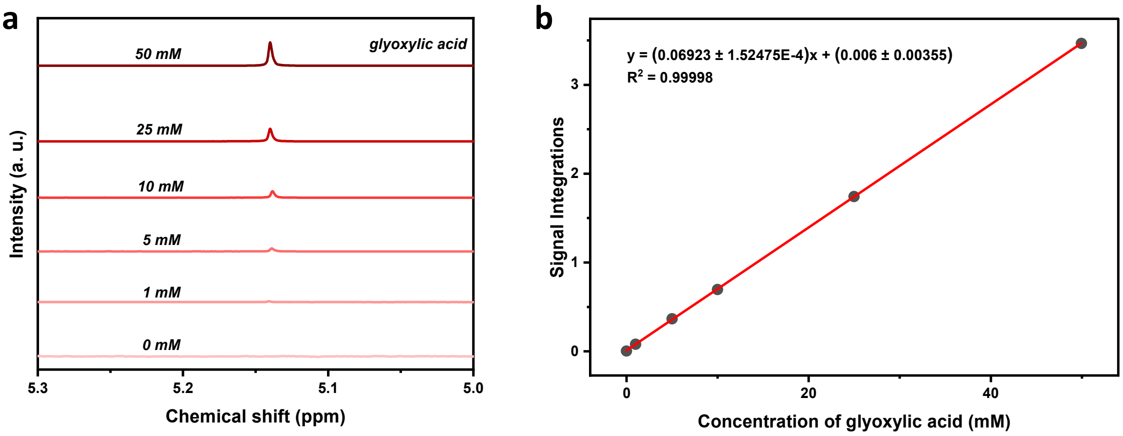

Figure S4. (a) ^{1}H NMR spectra and (b) associated ^{1}H NMR calibration curve of glyoxylic acid.

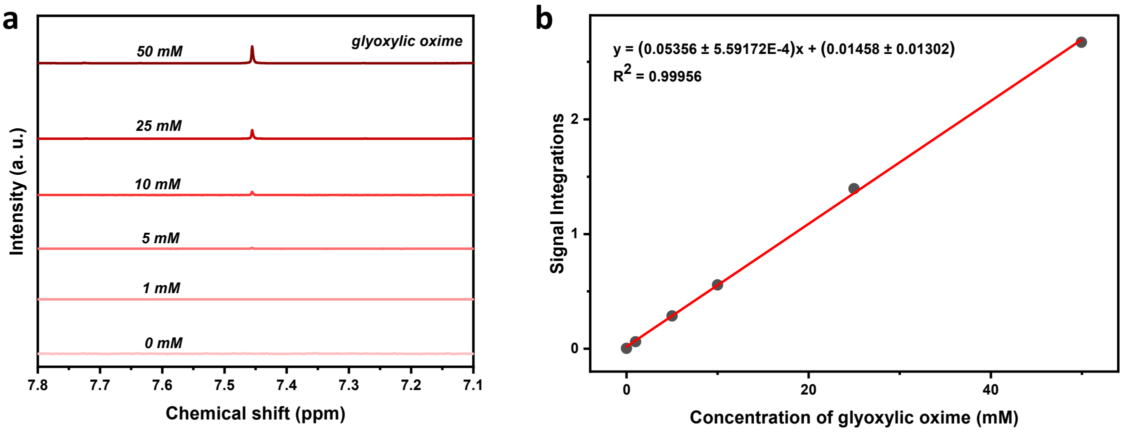

Figure S5. (a)^{1}H NMR spectra and (b) associated ^{1}H NMR calibration curve of glyoxylic oxime.

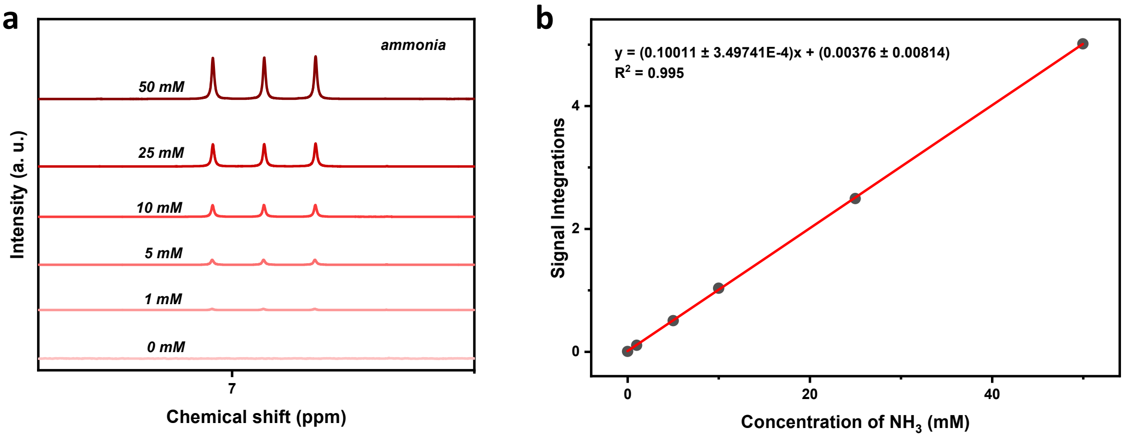

Figure S6. (a)^{1}H NMR spectra and (b) associated ^{1}H NMR calibration curve of ammonium.

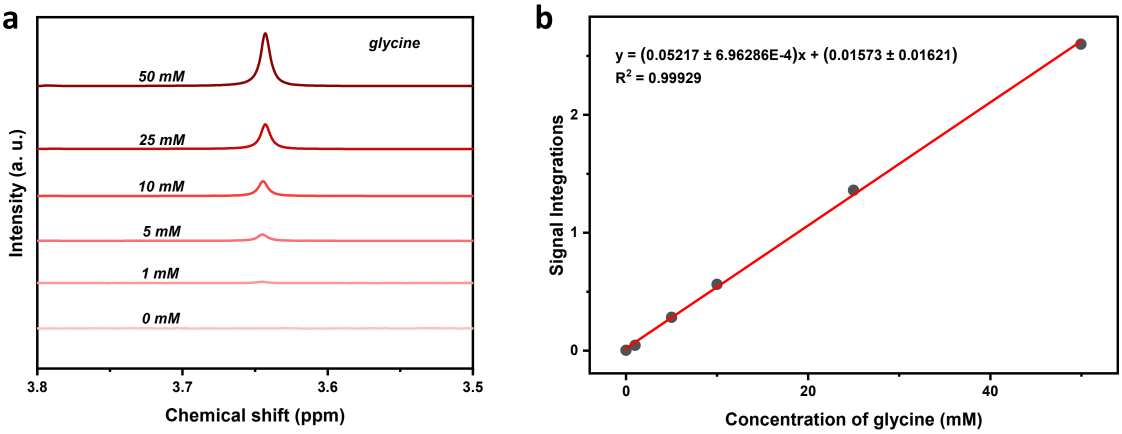

Figure S7. (a) ^{1}H NMR spectra and (b) associated ^{1}H NMR calibration curve of glycine.

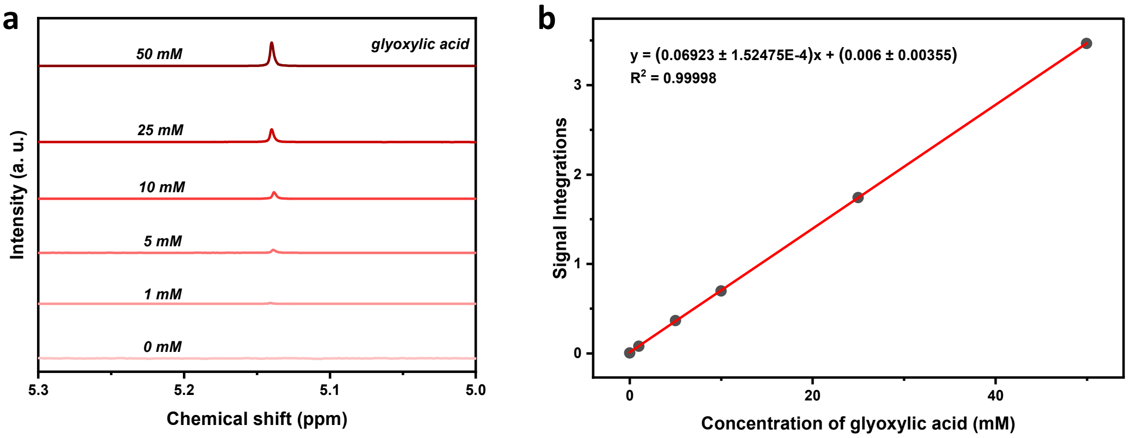

Figure S8. (a) ^{1}H NMR spectra and (b) associated ^{1}H NMR calibration curve of glycolic acid.

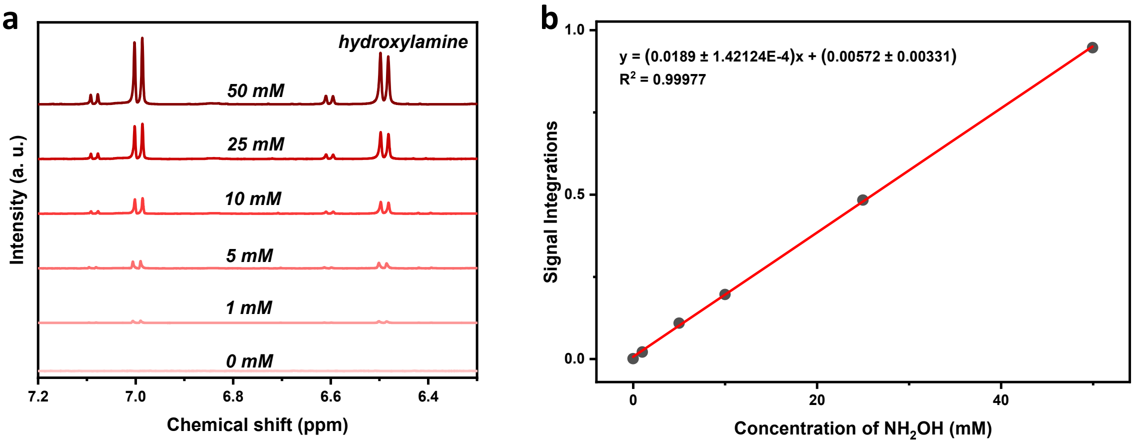

Figure S9. (a) ^{1}H NMR spectra and (b) associated ^{1}H NMR calibration curves of hydroxylamine.

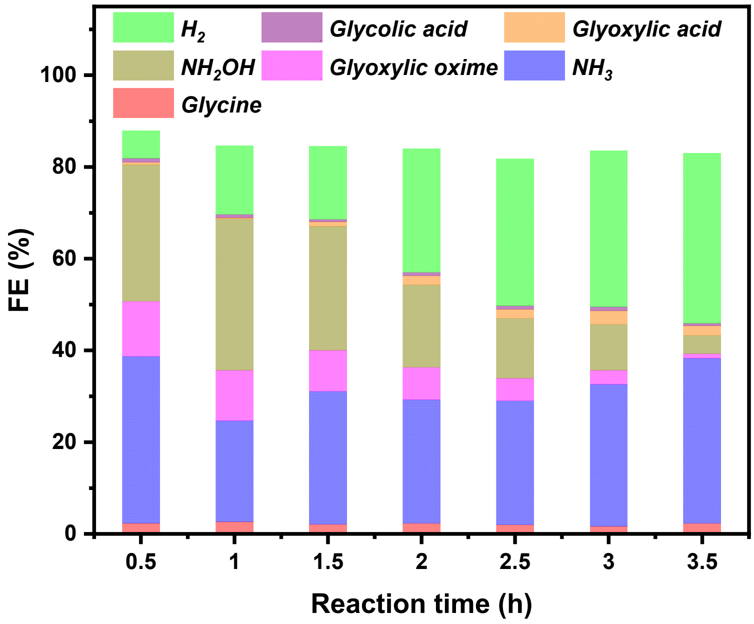

Figure S10. Time dependence of the faradaic efficiency for each product detected during a one-step tandem electrolysis at a constant current density of 200 mA cm^{-2} over the course of 3.5 h.

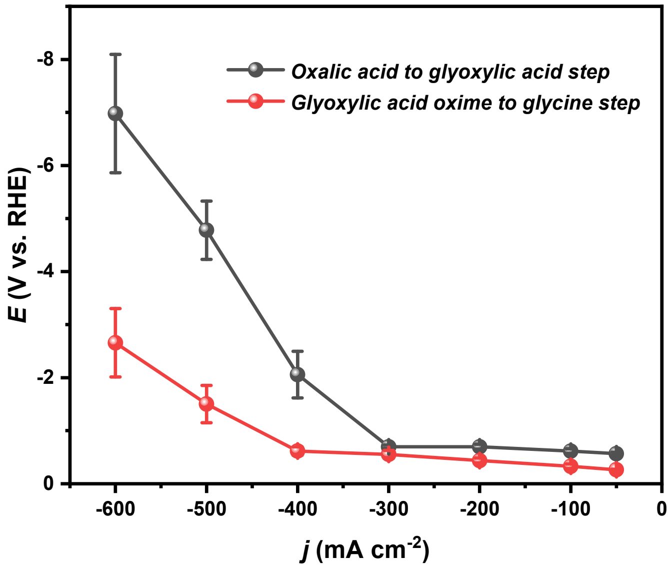

Figure S11. Steady-state polarization curves (E-*j*) for the first step of the tandem process (conversion of oxalic acid to glyoxylic acid, grey dots) and for the second step (glyoxylic acid to glycine, red dots) performed according to the two-step tandem (same *j*) electrolysis procedure (30 minutes for each step).

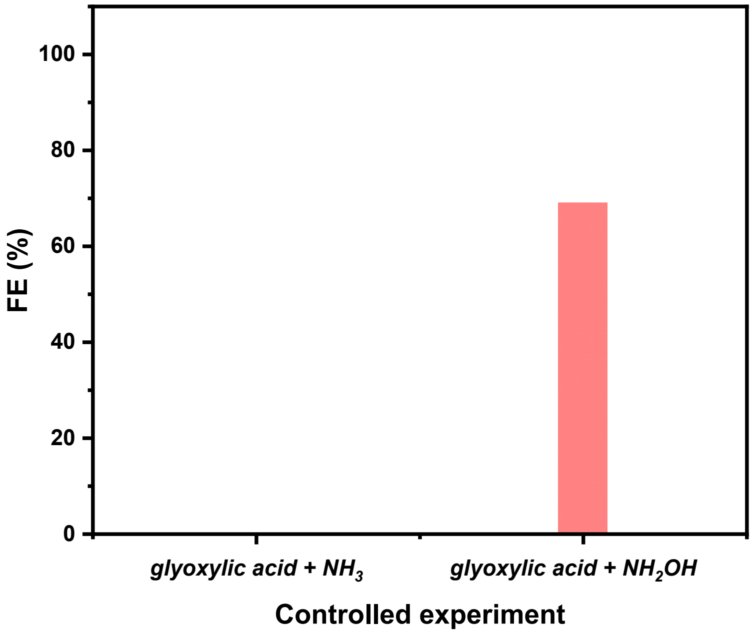

Figure S12. Glycine faradaic efficiency from the reduction of 0.5 M glyoxylic acid in the presence of either 0.5 M NH_3 or 0.5 M NH_2OH at a constant current density of -300 mA cm^{-2} for 30 minutes.

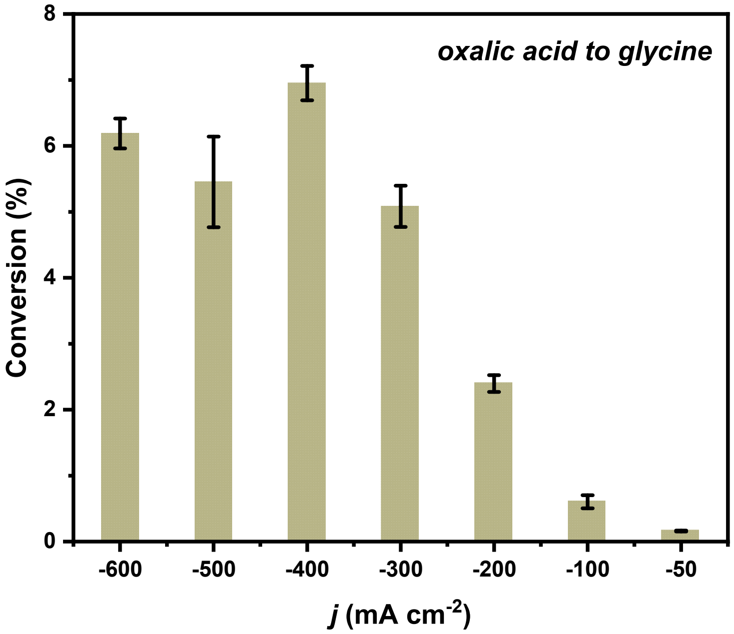

Figure S13. Conversion rate of oxalic acid to glycine following a two-step tandem (same j) electrolysis at various applied current densities (30 minutes for each step).

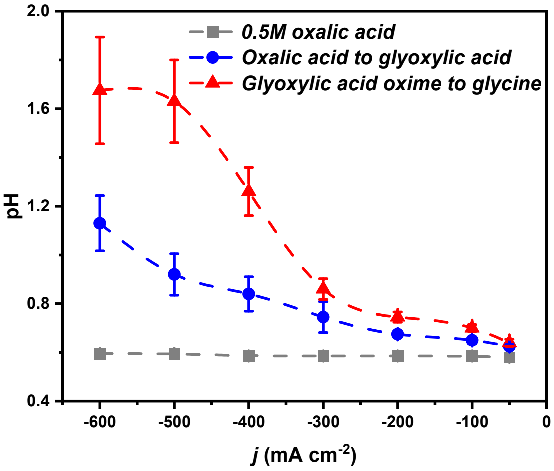

Figure S14. Evolution of catholyte pH values as a function of applied current density measured for difference stages of the tandem electrolysis: Fresh catholyte solutions (squares), catholytes after the oxalic acid to glyoxylic acid reduction step (circles), and catholytes after the glyoxylic acid oxime to glycine step (triangles). pH was measured after 30 minutes of electrolysis for each step.

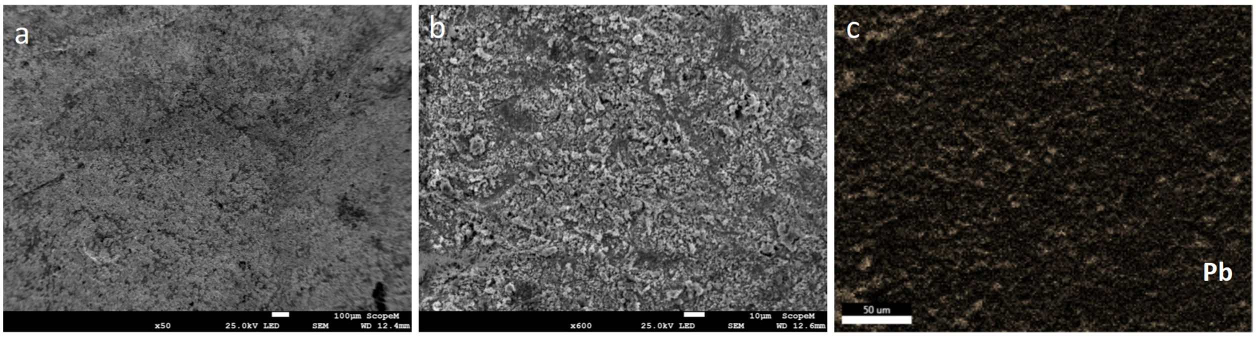

Figure S15. (a and b) SEM micrographs and the corresponding (c) EDX map of the Pb foil after applying -500 mA cm^{-2} for 5.5 hours during the oxalic acid to glyoxylic acid step, and -300 mA cm^{-2} for 20 hours during the glyoxylic acid to glycine step.

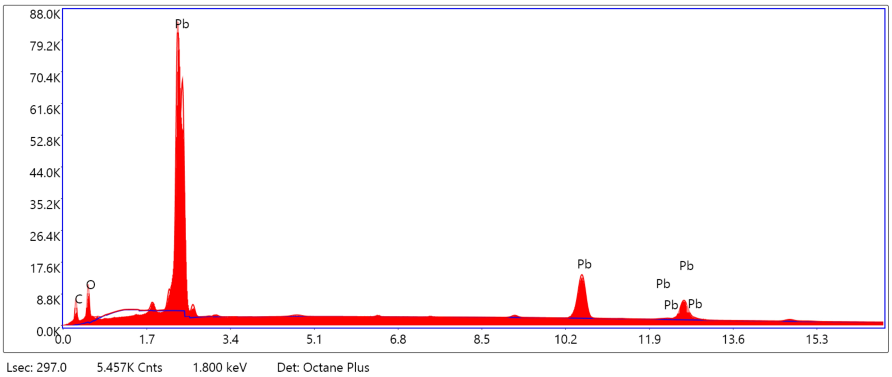

Figure S16. EDX spectrum of the Pb foil after applying -500 mA cm^{-2} for 5.5 hours during the oxalic acid to glyoxylic acid step, and -300 mA cm^{-2} for 20 hours during the glyoxylic acid to glycine step.

References

1. Y. Wu, Z. Jiang, Z. Lin, Y. Liang and H. Wang, *Nat. Sustain.*, 2021, **4**, 725-730.
2. X. Lan, C. Cheng, C. Guo, M. Guo, T. Li, Y. Wu, Y. Yu and B. Zhang, *Sci. China Chem.*, 2023, **66**, 1758-1762.
3. I. Katsounaros, *Curr. Opin. Electrochem.* , 2021, **28**, 100721.
4. V. Rosca, M. Duca, M. T. de Groot and M. T. Koper, *Chem. Rev.*, 2009, **109**, 2209-2244.
5. J. E. Kim, J. H. Jang, K. M. Lee, M. Balamurugan, Y. I. Jo, M. Y. Lee, S. Choi, S. W. Im and K. T. Nam, *Angew. Chem. Int. Ed.*, 2021, **133**, 22114-22122.
6. P. Li, K. Wang and B. Zhang, *ACS Appl. Mater. Interfaces*, 2024, **16**, 57171-57179.
7. K. Wang, P. Li and B. Zhang, *Appl. Catal. B: Environ.*, 2025, **361**, 124653.
8. L. Li, C. Wan, S. Wang, X. Li, Y. Sun and Y. Xie, *Nano Lett.*, 2024.
9. Y. Cheng, S. Liu, J. Jiao, M. Zhou, Y. Wang, X. Xing, Z. Chen, X. Sun, Q. Zhu and Q. Qian, *J. Am. Chem. Soc.*, 2024, **146**, 10084-10092.
10. P. J. Broersen, T. de Groot, D. F. Bruggeman, E. S. Caarls, J. A. Trindell, D. Anastasiadou, M. C. Figueiredo, G. Rothenberg and A. C. Garcia, *ChemCatChem*, 2024, **16**, e202301370.
11. T. Fukushima and M. Yamauchi, *Chem. Comm.*, 2019, **55**, 14721-14724.
12. Y. Xiao, C. W. Lim, J. Chang, Q. Yuan, L. Wang and N. Yan, *Green Chem.*, 2023, **25**, 3117-3126.
13. J. Xian, S. Li, H. Su, P. Liao, S. Wang, R. Xiang, Y. Zhang, Q. Liu and G. Li, *Angew. Chem. Int. Ed.*, 2023, e202306726.
14. T. Fukushima and M. Yamauchi, *J. Appl. Electrochem.*, 2021, **51**, 99-106.
15. M. Li, Y. Wu, B.-H. Zhao, C. Cheng, J. Zhao, C. Liu and B. Zhang, *Nat. Catal.*, 2023, **6**, 906-915.
16. J. Xian, S. Li, H. Su, P. Liao, S. Wang, Y. Zhang, W. Yang, J. Yang, Y. Sun and Y. Jia, *Angew. Chem. Int. Ed.*, 2023, **62**, e202304007.
17. K. Yan, M. L. Huddleston, B. A. Gerdes and Y. Sun, *Green Chem.*, 2022, **24**, 5320-5325.